Biomolecules and Biomedicine

ISSN: 2831-0896 (Print) | ISSN: 2831-090X (Online) Journal Impact Factor® (2024): 2.2

<u>CiteScore® (2024):</u> 5.2 <u>www.biomolbiomed.com</u> | blog.bjbms.org

SUPPLEMENTAL DATA

Mitochondrial dysfunction triggers Zbp1-mediated necroptosis and inflammation in acute lung injury

Mi Zhou¹, Yuehan Li¹, Yinying Ren¹, Yan Li¹, JinYing Xiang¹, Fang Deng¹, Gang Geng¹, Jian Luo¹, Jinyue Yu^{2,3}, Zhou Fu¹, Fengxia Ding^{1*}, Bo Liu^{4*}

¹Department of Pediatric Respiratory Medicine; National Clinical Research Center for Child Health and Disorders; Ministry of Education Key Laboratory of Child Development and Disorders; China International Science and Technology Cooperation Base of Child Development and Critical Disorders; Chongqing Engineering Research Center of Stem Cell Therapy, Children's Hospital of Chongqing Medical University, Chongqing, China;

²Bristol Medical School, University of Bristol, Bristol, UK;

³Great Ormond Street Institute of Child Health, University College London, London, UK;

⁴Department of Pediatric Cardiothoracic Surgery; National Clinical Research Center for Child Health and Disorders; Ministry of Education Key Laboratory of Child Development and Disorders; China International Science and Technology Cooperation Base of Child Development and Critical Disorders; Chongqing Engineering Research Center of Stem Cell Therapy, Children's Hospital of Chongqing Medical University, Chongqing, China.

*Correspondence to Fengxia Ding: <u>482613@hospital.cqmu.edu.cn</u> and Bo Liu: <u>lbcqmu@126.com</u>.

Full article is available at the following link: Mitochondrial dysfunction triggers

Zbp1-mediated necroptosis and inflammation in acute lung injury

Ethical statement

All experimental procedures involving animals adhered strictly to ethical guidelines and were conducted in compliance with the principles outlined in the National Institutes of Health Guide for the Care and Use of Laboratory Animals. The study protocol received formal approval from the Ethics Committee of Children's Hospital of Chongqing Medical University (Approval No. CHCMU-IACUC20220804007).

Experimental animals

Female C57BL/6 wild-type mice (6–8 weeks old) were sourced from the Animal Experiment Center of Chongqing Medical University. Mice were housed under standard conditions, including a 12-hour light/dark cycle, and provided with a standard diet and ad libitum access to water in the Animal Experimental Center of the Children's Hospital of Chongqing Medical University.

The mice were randomly divided into two groups (n = 3 per group) using a random number table: the normal control group and the experimental group. There were no significant differences in body weight or age between the groups at baseline. To establish an acute lung injury (ALI) model, mice were anesthetized with an intraperitoneal injection of pentobarbital (50 mg/kg). After the skin and muscle were carefully incised to expose the trachea, 70 μ L of lipopolysaccharide (LPS; 1 mg/kg; Solarbio Technology, China) was administered intratracheally using a microinjector. The incision was then sutured, and the mice were monitored. After 36 hours, mice were euthanized, and lung tissues were collected for subsequent analyses.

Assessment of lung inflammation

Bronchoalveolar lavage fluid (BALF) was obtained by flushing the lungs three times with pre-cooled PBS (0.5 mL per lavage). After centrifugation, cell pellets were lysed using a red blood cell lysis buffer and counted using an automated cell counter. The supernatant BALF was analyzed for protein concentration via a bicinchoninic acid (BCA) assay to evaluate pulmonary vascular leakage.

Cytokine levels (IL-1β, IL-6, IL-10, and TNF-α) in BALF were measured using ELISA kits (Fine Test, China) according to the manufacturer's instructions. Absorbance was read at 450 nm using an Epoch microplate reader (BioTek, USA).

Myeloperoxidase (MPO) activity in lung tissues was quantified using an MPO detection kit (Solarbio, China) following the provided protocol. Lung water content was calculated as the ratio of wet-to-dry lung weight. Wet weight was recorded after harvesting the left lung, which was then dried at 60 °C for 48 hours to determine the dry weight.

Transmission electron microscopy (TEM)

Samples were fixed in 2.5% glutaraldehyde for 4 hours, followed by post-fixation with 1% osmium tetroxide (OsO₄) for an additional 4 hours. Dehydration was performed using a graded ethanol series and propylene oxide. Samples were embedded in resin and ultra-thin sections (70 nm) were cut. Sections were stained with uranyl acetate and lead citrate for 8 minutes each and imaged using a transmission electron microscope (JEM-1400FLASH, Japan).

Hematoxylin and Eosin (H&E) staining

Lung tissues were fixed in 4% paraformaldehyde (PFA) for 24 hours, dehydrated, and embedded in paraffin. Sections (4 µm thick) were dewaxed, rehydrated, and stained with hematoxylin and eosin (H&E). After staining, sections were dehydrated through a graded alcohol series, cleared in xylene, and mounted with neutral gum. The lung injury score was determined following a previously established methodology^[33] by an investigator blinded to the experimental groups. The scoring system evaluates inflammation in the trachea, bronchioles, perivascular areas, and lung interstitium. Inflammation severity in each of these regions was graded on a scale from 1 to 3, where 1 indicates mild inflammation, 2 indicates moderate inflammation, and 3 indicates severe inflammation.

Terminal deoxynucleotidyl transferase dUTP Nick-End labeling (TUNEL) staining

Lung tissue sections were stained using a TUNEL assay kit (Elabscience, China) according to the manufacturer's protocol. Briefly, sections were dewaxed, rehydrated, and permeabilized with proteinase K working solution was applied, followed by counterstaining with DAPI. After mounting with anti-fade reagent, fluorescence imaging was performed to assess lung tissue damage.

Immunofluorescence histochemistry

Lung tissues fixed in 4% PFA were dehydrated, embedded in paraffin, and sectioned (4 μm thick). After dewaxing and rehydration, antigen retrieval was performed using Tris buffer. Sections were permeabilized with 0.1% Triton X-100 for 10 minutes, blocked with 5% bovine serum albumin (BSA), and incubated overnight at 4 °C with primary antibodies: Zbp1 (cat.#:13285-1-AP, Proteintech, China; dilution 1:100) and p-RIPK3 (cat.#:91702, CST, USA, dilution 1:100). The following day, FITC-labeled goat anti-rabbit IgG secondary antibody (cat.#:A0562, Beyotime, China; dilution 1:250) were applied for 1 hour in the dark.

For subsequent staining, sections were blocked with 5% BSA and incubated overnight with TOMM20 (cat.#:382451, ZEN-BIO, China, dilution1:100). Cy3-labeled goat anti-rabbit IgG secondary antibody (cat.#: A1623, Beyotime, China; dilution 1:250) were applied. APC-conjugated anti-mouse Siglec-F antibody (cat.#: AN00629E, Elabscience, China; dilution 1:200) were used for an additional overnight incubation. Nuclei were stained with DAPI for 10 minutes at room temperature. After mounting with an anti-fade reagent, imaging was conducted using a laser scanning confocal microscope (Nikon, Japan).

RESULTS

LPS-induced Zbp1-mediated necroptosis and pulmonary inflammation in a murine ALI model

To systematically evaluate LPS-induced pulmonary damage in a murine model of ALI, a comprehensive series of assays was conducted. The wet-to-dry (W/D) weight ratio of lung tissue, an indicator of pulmonary edema, showed a significant increase in LPS-treated mice compared to controls (Figure S4A). Similarly, myeloperoxidase (MPO) activity, a marker of neutrophil infiltration, was markedly elevated in lung homogenates from LPS-exposed mice (Figure S4B). Bronchoalveolar lavage fluid (BALF) analysis further corroborated the presence of pulmonary injury. Cell counts and protein concentration in BALF, reflective of alveolar-capillary membrane permeability and inflammation, were significantly elevated in LPS-treated mice (Figure S4C-D). ELISA of BALF revealed substantially increased levels of proinflammatory cytokines, including TNF-α, IL-10, IL-6, and IL-1β, compared to the

control group (Figure S4E–H). These findings highlight the severe inflammatory response and disruption of the alveolar-capillary barrier in LPS-induced ALI. TEM provided ultrastructural insights into alveolar macrophages, focusing on mitochondrial morphology. In the control group, mitochondria within alveolar macrophages exhibited dense matrices and well-defined cristae. In contrast, LPSexposed mice displayed significant mitochondrial abnormalities, including reduced matrix density, loss of cristae integrity, and pronounced vacuolization (Figure S4I). Histopathological analysis via H&E staining revealed substantial inflammatory cell infiltration, the formation of hyaline membranes, and elevated inflammatory injury scores in lung sections from LPS-treated mice, indicative of severe pulmonary inflammation and tissue damage (Figure S4J-K). Additionally, TUNEL staining demonstrated increased apoptotic activity in lung tissue from ALI mice, suggesting a contribution of cell death to the disease pathophysiology (Figure S4L-M). Immunofluorescence was employed to identify specific cellular and molecular mechanisms underlying ALI. Alveolar macrophages were labeled with SiglecF, while mitochondrial components were marked with TOMM20. To investigate Zbp1mediated necroptosis, antibodies against Zbp1 and p-RIPK3 were utilized. Results showed elevated expression of Zbp1 and p-RIPK3 in alveolar macrophages from LPS-treated mice, with significant colocalization observed between these markers and mitochondrial structures (Figure S4N-Q). These findings suggest that the Zbp1mediated necroptosis pathway is activated in LPS-induced ALI and is closely associated with mitochondrial dysfunction in alveolar macrophages, potentially playing a critical role in the pathogenesis of ALI.

Table S1. Primer sequences used for qRT-PCR

Primers	Base sequence(5'to3')
M-Zbp1-R	AGGCGGTAAAGGACTTGATTGAG
M-Zbp1-F	GTTGACTTGAGCACAGGAGACA
M-β-actin-R	ATGCCACAGGATTCCATACC
M-β-actin-F	GTGCTATGTTGCTCTAGACTTCG
M-18S-R	CGCTGAGCCAGTCAGTGT
M-18S-F	TAGAGGGACAAGTGGCGTTC
M-TNFa-R	GCCATAGAACTGATGAGAGGGAG
M-TNFa-F	GGTGCCTATGTCTCAGCCTCTT
M-IL-1β-R	GTTCATCTCGGAGCCTGTAGTG
M-IL-1β-F	TGGACCTTCCAGGATGAGGACA
M-IL6-F	TACCACTTCACAAGTCGGAGGC
M-IL6-R	CTGCAAGTGCATCATCGTTGTTC

Table S2. The sequences of siRNA primers

Primers	Base sequence(5'to3')
Zbp1 Mouse Pre-designed siRNA-	CCUAGCCUUGAUGAAAGAAUAdTdT
1	
	UAUUCUUUCAUCAAGGCUAGGdTdT
Zbp1 Mouse Pre-designed siRNA-	CCUGUAUUCCAUGAGAAAUAAdTdT
2	
	UUAUUUCUCAUGGAAUACAGGdTdT
Zbp1 Mouse Pre-designed siRNA-	GCGAUUAUUUGUCAGCACAAUdTdT
3	
	AUUGUGCUGACAAAUAAUCGCdTdT

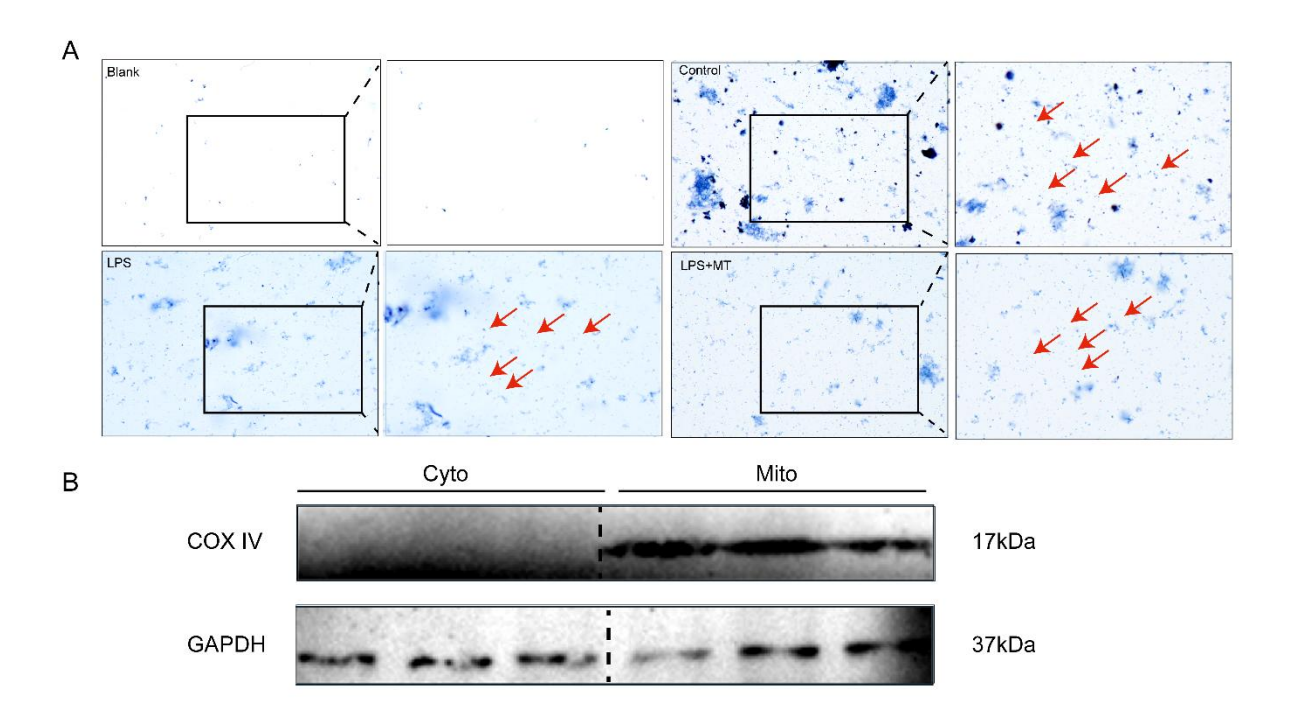


Figure S1. Validation of isolated mitochondria. (A) Representative images of mitochondria stained with Janus green B and observed under a light microscope (20x objective). (B) Western blot analysis of COX IV and GAPDH expression in the cytosolic and mitochondrial fractions. Abbreviation: GAPDH: Glyceraldehyde-3-phosphate dehydrogenase.

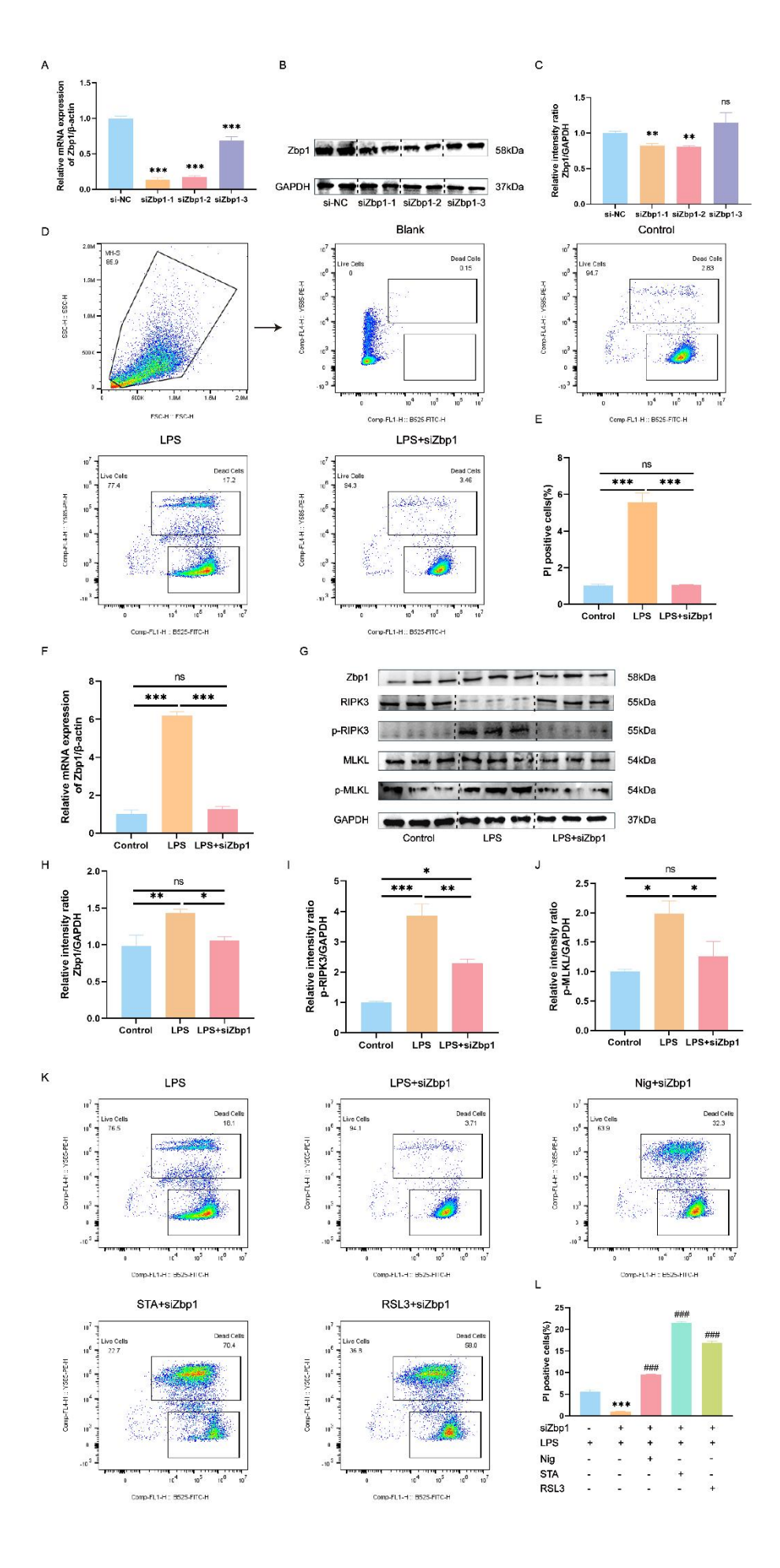


Figure S2. Attenuation of LPS-induced necroptosis in MH-S cells by Zbp1

knockdown. (A) qRT-PCR analysis of Zbp1 mRNA levels in cells transfected with different siRNA sequences, with β -actin serving as an internal control. ***p < 0.001vs si-NC group. (B) Western blot analysis of Zbp1 protein expression following transfection with the indicated siRNA sequences. GAPDH was used as a loading control. (C) Densitometric quantification of the Western blot results for Zbp1 from panel (B). **p < 0.01 vs si-NC group, "ns" indicates not significant versus si-NC. (D-E) Assessment of cell death by flow cytometry in Zbp1-knockdown MH-S cells using Calcein/PI staining. ***p < 0.001, "ns" indicates no significance. (F) Analysis of Zbp1 mRNA levels via qRT-PCR in Zbp1-knockdown MH-S cells, normalized to βactin. ***p < 0.001, "ns" indicates no significance. (G) Western blot analysis of Zbp1, p-RIPK3, and p-MLKL protein expression in Zbp1-knockdown MH-S cells. (H-J) Quantitative densitometry analysis of the corresponding protein bands from (G). *p <0.05, **p < 0.01, ***p < 0.001, "ns" indicates no significance. (K-L) Flowcytometric analysis of cell death (by Calcein/PI staining) in Zbp1-knockdown MH-S cells following treatment with specific inducers of pyroptosis (Nigericin), apoptosis (Staurosporine), or ferroptosis (RSL3). Nig means Nigericin, STA means Staurosporine, ***p <0.001 vs LPS+si-NC group, ### p <0.001 vs LPS+siZbp1 group. Data are presented as mean \pm SEM, n \geq 3. Normality was assessed using the Shapiro-Wilk test. For one-way ANOVA, Tukey's test was subsequently used for multiple comparisons. Abbreviations: LPS: Lipopolysaccharide; MH-S: Murine alveolar macrophage-like cell line; GAPDH: Glyceraldehyde-3-phosphate dehydrogenase; PI: Propidium iodide; RIPK3: Receptor-interacting protein kinase 3; p-RIPK3: Phosphorylated receptor-interacting protein kinase 3; MLKL: Mixed lineage kinase domain-like protein; p-MLKL: Phosphorylated mixed lineage kinase domain-like protein; Nig: Nigericin; STA: Staurosporine; SEM: Standard error of the mean; ANOVA: Analysis of variance.

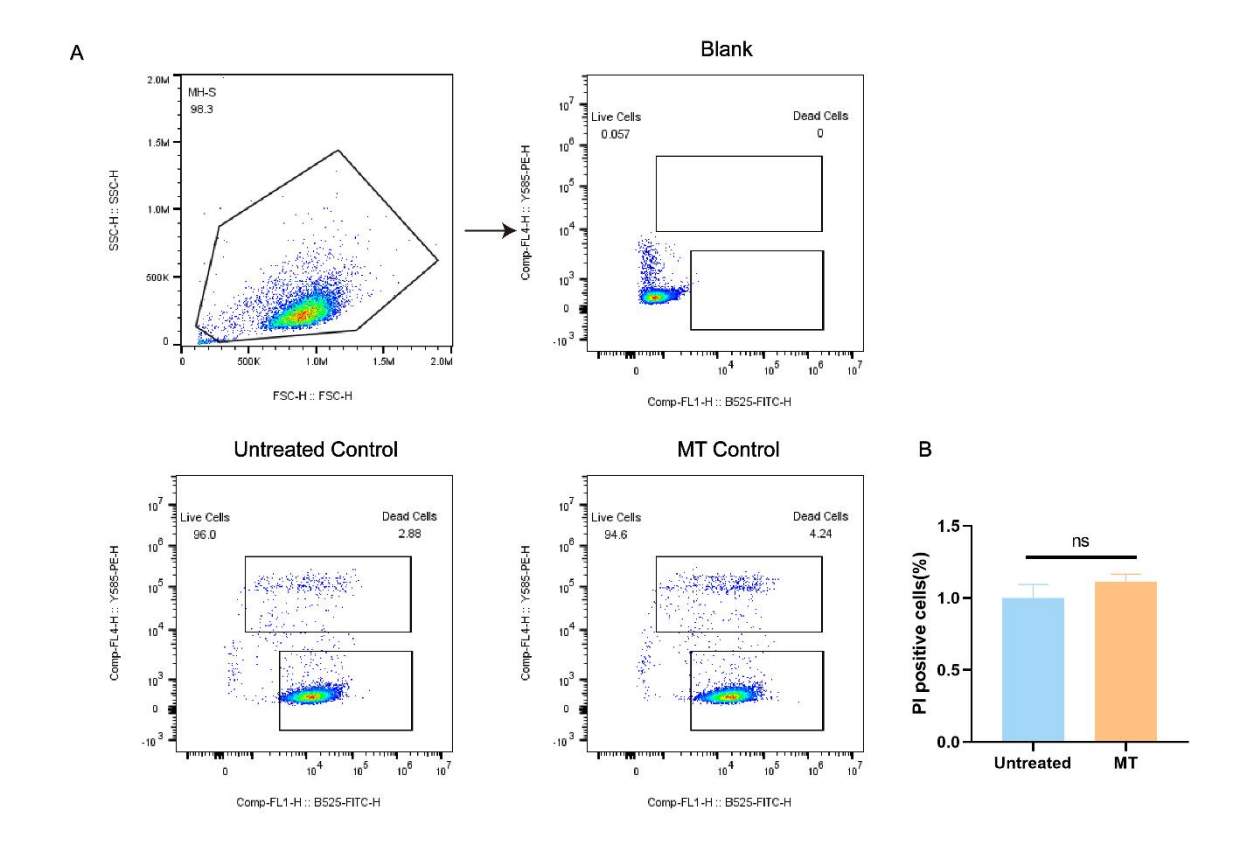


Figure S3. Flow cytometric analysis with calcein/PI staining: Untreated control versus Mito-TEMPO (MT) control. (A) Representative flow cytometry plots from Calcein/PI staining of Untreated Control and MT Control groups. (B) Quantitative analysis of PI-positive cells between the Untreated Control and MT Control groups. Data are presented as mean \pm SEM, $n \ge 3$. Normality was assessed using the Shapiro-Wilk test. Unpaired two-tailed Student's t-test for comparisons between two groups; "ns" indicates not significant. Abbreviations: PI: Propidium iodide; SEM: Standard error of the mean.

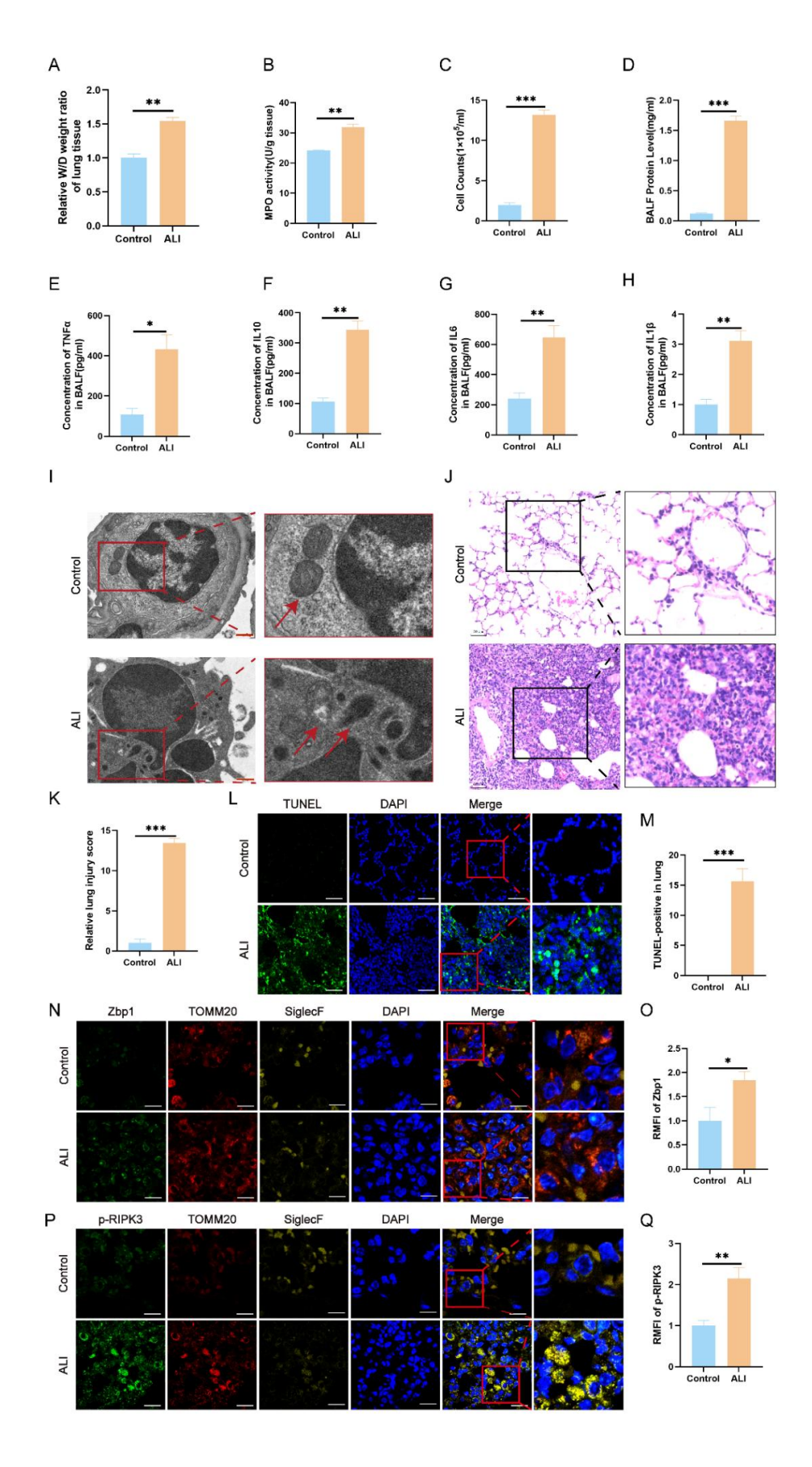


Figure S4. LPS-induced necroptosis and pulmonary inflammation in a murine ALI model. (A) W/D weight ratio analysis of ALI lung tissue. N=3 (B) MPO activity

assay in lung homogenates. N=3 (C) Cell counts in BALF. N=3 (D) Quantification of total protein concentration in BALF. N=3 (E-H) Measurement of cytokine levels in BALF using ELISA, including TNF-α, IL-10, IL-6, and IL-1β. N=3 (I) TEM imaging of alveolar macrophages in lung tissue. Scale bar = 500 nm. (J) H&E staining of lung tissue for histopathological evaluation. Scale bar = 50 µm. (K) Lung injury scoring based on histological assessment of lung tissue. (L-M) TUNEL staining for the detection of apoptotic cells and calculation of the proportion of TUNEL-positive cells in lung tissue. Scale bar = $25 \mu m$. (N) Immunofluorescence imaging of Zbp1, TOMM20, and SiglecF in lung tissue. (O) RMFI of Zbp1 in lung tissue. (P) Immunofluorescence imaging of p-RIPK3, TOMM20, and SiglecF in lung tissue. (Q) Representative mean fluorescence intensity (RMFI) of p-RIPK3 in lung tissue. Data were presented as the mean \pm SEM and analyzed by unpaired t test; *p < 0.05, **p < 0.01, ***p < 0.001, "ns" indicates not significant. Abbreviations: ALI: Acute lung injury; MPO: Myeloperoxidase; BALF: Bronchoalveolar lavage fluid; TNF-α: Tumor necrosis factor alpha; TEM: Transmission electron microscopy; H&E: Hematoxylin and eosin; TOMM20: Translocase of outer mitochondrial membrane 20; RMFI: Relative mean fluorescence intensity; p-RIPK3: Phosphorylated receptor-interacting protein kinase 3; SEM: Standard error of the mean.